Synthesis, Characterization, and Theoretical Studies of the New Antibacterial Zn(II) Complexes from New Fluorescent Schiff Bases Prepared by imidazo[4',5':3,4]benzo[1,2-*c*]isoxazole

Nakhaei, Ahmad*[+]

Young Researchers and Elite Club, Mashhad Branch, Islamic Azad University, Mashhad, I.R. IRAN

Ramezani, Shirin

Department of Chemistry, Mashhad Branch, Islamic Azad University, Mashhad, I.R. IRAN

ABSTRACT: *The novel fluorescent heterocyclic bidentate ligands have been synthesized by the high yields reaction of 8-(4-chlorophenyl)-3-Iso-butyl-3H-imidazo[4',5':3,4]benzo[1,2-c]isoxazol-5-amine with p-hydroxybenzaldehyde and p-chlorobenzaldehyde. The ligands reacted with Zn(II) ion to gained novel complexes. The optical properties of these structures were checked and the outcomes represented that they showed interesting photophysical properties. Optimized geometries and assignment of the IR bands and NMR chemical shifts of the new complexes were also computed by using Density Functional Theory (DFT) methods that were in good agreement with the experimental values, confirming the suitability of the optimized geometries for Zn(II) complexes. These new compounds have shown potent antibacterial properties and their antibacterial activity (MIC) against Gram-positive and Gram-negative bacterial species were also specific.*

KEYWORDS: *Zn(II) complex; Antibacterial activity; Schiff base; Bidentate ligand; Density Functional Theory (DFT).*

INTRODUCTION

Zinc complexes have received considerable attention owing to their effective biological importance such as antibacterial [1] antifungal [2] antivirus [3] antiproliferative [4] and anticancer activity [5]. The stabilities and coordination chemistry of zinc (II) with bidentate ligands [6] have also resulted from their efficacy as oral zinc chelating agents [7] and as agents for the treatment of zinc overload conditions [8].

Benzo[1,2-*c*]isoxazoles are an important class of heterocyclic pharmaceuticals and bioactive compounds that are prescribed as antipsychotic risperidone [9] and anti-HIV drugs [10] and play a key role in many organic reactions [11]. Isoxazole-metal complexes are often postulated as intermediates in reactions of considerable synthetic utility, for example the reductive ring opening of isoxazoles. Several isoxazole-metal complexes

* *To whom correspondence should be addressed.*

+ E-mail: nakhaei_a@yahoo.com ; nakhaei_a@mshdiau.ac.ir

1021-9986/2019/4/79-90 12/$/6.02

have been reported and well characterized. In a review of the literature of isoxazole-metal complexes [12], the binding characteristics of the isoxazoles in the complexes have been examined, and some tentative conclusions regarding the regularity of isoxazole complexation behavior have been discussed.

On the other hand, Schiff bases are an important class of organic ligands, due to their biological properties [13]. Schiff bases have many advantages between ligands in the coordination chemistry. They are the most versatile studied ligands in coordination chemistry because of their structural varieties and very unique characteristics. These findings promoted us to synthesis and characterization of two new fluorescent heterocyclic Schiff-base ligands derived from 2-8-(4-chlorophenyl)-3-Iso butyl -3*H*-imidazo[4',5':3,4]benzo [1,2-*c*]isoxazol-5-amine and their Zn (II) complexes. In addition, antibacterial activities of the new ligands and complexes against gram positive and negative bacterial species were studied.

EXPERIMENTAL SECTION

Equipment and Materials

Melting points were measured on an Electrothermaltype-9100 melting-point apparatus. The FT-IR (as KBr discs) spectra were obtained on a Tensor 27 spectrometer and only noteworthy absorptions are listed. The ^{13}C NMR (100 MHz) and ^{1}H NMR (400 MHz) spectra were recorded on a Bruker Avance DRX-400 spectrometer. Chemical shifts are reported in ppm downfield from TMS as internal standard; coupling constant *J* is given in Hz. The mass spectrum was recorded on a Varian Mat, CH-7 at 70 eV and ESI mass spectrum was measured using a Waters Micromass ZQ spectrometer. Elemental analysis was performed on a Thermo Finnigan Flash EA microanalyzer. Absorption and fluorescence spectra were recorded on Varian 50-bio UV-Visible spectrophotometer and Varian Cary Eclipse spectrofluorophotometer. UV–vis and fluorescence scans were recorded from 200 to 1000 nm. Percentage of the Zn^{+2} ion was obtained by using a Hitachi 2-2000 atomic absorption spectrophotometer.

The microorganisms *Bacillus subtilis* ATCC 6633, *Pseudomonas aeruginosa* ATCC 27853 and *Escherichia coli* ATCC 25922 were purchased from Pasteur Institute of Iran and *S. aureus* methicillin resistant was isolated from different specimens which were referred to the Microbiological Laboratory of Ghaem Hospital of Medical University of Mashhad, Iran, and its methicillin resistance was tested according to the NCCLS guidelines [14]. All solvents were dried according to standard procedures. Compounds **1** [15]**, 3** [16], **4** [17] and **5a** [18] were obtained according to the published methods. Other reagents were commercially available.

Computational methods

All of the calculations have been performed using the DFT method with the B3LYP functional [19] as implemented in the Gaussian 03 program package [20]. The 6-311+G(d,p) basis sets were employed except for the Zn atom where the LANL2DZ basis sets were used with considering its effective core potential. Geometry of the Zn complex was fully optimized, which was confirmed to have no imaginary frequency of the Hessian. Geometry optimization and frequency calculation simulate the properties in the gas/solution phases.

The fully-optimized geometries were confirmed to have no imaginary frequency of the Hessian.

The solute-solvent interactions have been investigated using one of the self-consistent reaction field methods, i.e., the sophisticated Polarizable Continuum Model (PCM) [21].

General procedure for the synthesis of 7a,b from 5a

Aldehyde **6a,b** (1 mmol) was added to a solution of compound **5a** (0.34 g, 1 mmol) in ethanol (15 mL). The reaction mixture was heated under reflux for 5 hours. The solvent was removed under reduced pressure and the yellow product was filtered and washed with ethanol to give Schiff base (**7a,b**), which was purified in hot acetone.

E)-4- (((8-(4-chlorophenyl) -3-isobutyl- 3H-imidazo [4',5':3,4]benzo[1,2-c]isoxazol-5-yl)imino)methyl)phenol (**7a, L1**) was obtained as a yellow powder. m.p: 175-179 °C. ^{1}H NMR ($CDCl_3$): δ 0.92 (d, J = 6.4 Hz, 6 H), 2.21–2.25 (m,1 H), 4.37 (d, J = 7.2 Hz, 2 H), 6.95 (d, *J* = 8.4 Hz, 2H, Ar H), 7.69 (s, 1H, Ar H), 7.73 (d, *J* = 8.4 Hz, 2H, Ar H), 7.87 (d, *J* = 8.7 Hz, 2H, Ar H), 8.31 (s, 1H, Ar H), 8.95 (d, *J* = 8.7 Hz, 2H, Ar H), 9.08 (s, 1H, CH), 10.37 (br s, 1H, OH) ppm; ^{13}C NMR ($CDCl_3$): δ 21.4, 29.2, 57.8, 114.5, 114.8, 121.5, 131.7, 132.3, 133.6, 134.8,

135.3, 135.5, 136.3, 140.2, 140.8, 147.2, 158.7, 165.2, 166.3, 166.8 ppm. IR (KBr): 3357 cm^{-1} (OH), 1652 cm^{-1} (CH=N).

(E)-N-(4-chlorobenzylidene) -8-(4-chlorophenyl) -3-isobutyl-3H-imidazo [4',5':3,4] benzo[1,2-c]isoxazol-5-amine (**7b, L2**) was obtained as a yellow powder. m.p: 189–193 °C; yield: 75%. ^{1}H NMR ($CDCl_3$): δ 0.92 (d, J = 6.4 Hz, 6 H), 2.01–2.05 (m,1 H), 4.26 (d, *J* = 7.2 Hz, 2 H), 7.64 (d, *J* = 8.4 Hz, 2H, Ar H), 7.68 (d, *J* = 8.7 Hz, 2H, Ar H), 7.71 (s, 1H, Ar H), 7.88 (d, *J* = 8.4 Hz, 2H, Ar H), 8.29 (s, 1H, Ar H), 8.82 (d, *J* = 8.7 Hz, 2H, Ar H), 9.21 (s, 1H, CH=N) ppm; ^{13}C NMR ($CDCl_3$): δ 19.8, 32.6, 44.9, 110.2,112. 1, 127.1, 129.3, 129.7, 129.9, 130.1, 130.5, 131.7, 131.9, 134.3, 135.7, 135.9, 136,5, 143.4, 154.8, 162.3, 162.5 ppm. IR (KBr): 1664 cm^{-1} (CH=N).

General procedure for the synthesis of complexes 8a,b from ligands 7a,b

To the yellow solution of ligand **7a,b** (2 mmol) in aqueous metanolic solution (20 mL**,** MeOH, H_2O, 10:90) Zn (II) nitrate hexahydrate (0.29 gr, 1 mmol) was added, resulting in color change to deep green. The reaction was carried out for another 6 h in room temperature. The complex was isolated by evaporation of the solvent and washed with cold MeOH and then H_2O.

c[$Zn(L1)_2$]N_2O_6.2(H_2O)] (**8a**): was obtained as a dark green powder. mp > 300 ºC (decomp). ^{1}H NMR (DMSO-*d6*): δ 0.89 (t, *J* = 6.4 Hz, 12H, CH_3), 1.71–1.74 (m, 2H, CH), 4.33 (t, *J* = 7.2 Hz, 4H, NCH_2), 7.12 (d, *J* = 9.0 Hz, 4H, Ar H), 7.75–7.95 (m, 10H, Ar H), 8.36 (s, 2H, Ar H), 8.94 (d, *J* = 9.0 Hz, 4H, Ar H), 9.21 (s, 2H, CH), 10.78 (br s, 2H, OH). IR (KBr): 3371 cm^{-1} (OH), ESI-MS (+) m/z (%): 990 $[Zn(L2)_2]^{2+}$. Anal. Calcd for $C_{50}H_{46}Cl_2N_{10}O_{12}$ Zn (1115.2): C, 53.85; H, 4.16; N, 12.56; Zn, 5.86. Found: C, 53.27; H, 4.01; N, 11.94; Zn, 5.09.

[$Zn(L2)_2$].N_2O_6 2(H_2O) (**8b**): was obtained as a dark green powder. mp > 300 ºC (decomp). IR (KBr): 3435, cm^{-1} (OH), ESI-MS (+) m/z (%): 954 $[Zn(L1)_2]^{2+}$. Anal. Calcd for $C_{50}H_{44}Cl_4N_{10}O_{10}Zn$ (1152.1): C, 52.12; H, 3.85; N, 12.16; Zn, 5.68. Found: C, 51.92; H, 3.71; N, 11.36; Zn, 5.42.

RESULTS AND DISCUSSION

Synthesis and structure of the new ligands 7a,b and complexes 8a,b

In order to the synthesis of new heterocyclic Schiff-base ligands, the commercially available 5-nitro-1*H*-benzimidazole was alkylated with 1-Bromo-2-methylpropane in KOH and DMF to produce 1-iso-butyl-5-nitro-1*H*-benzimidazole (**1a)** [15]. 3-Iso-butyl-8-(4-chlorophenyl)-3*H*-imidazo [4',5':3,4]benzo[1,2-*c*]isoxazoles (**3a)** was prepared from the reaction of 1-iso-butyl-5-nitro-1*H*-benzimidazole **1a** with (4-chlorophenyl) acetonitrile (**2a)** in basic MeOH solution [16]. Regioselective nitration of **3a** was accomplished using a mixture of sulfuric acid and potassium nitrate and led to the formation of 3-iso-butyl-8-(4-chlorophenyl)-5-nitro-3*H*-imidazo[4',5':3,4]benzo[1,2-*c*]isoxazole **4a** in good yield [17, 22]. Reduction of compounds **4a** in EtOH by $SnCl_2$, gave the 8-(4-chlorophenyl)-3-iso-butyl-3*H*-imidazo[4',5':3,4]benzo[1,2-*c*]isoxazol-5-amine (**5a**) in high yields. Finally, new heterocyclic Schiff-bases **7a,b** were synthesized by the reaction of amines **5a** with aldehydes **6a,b** in good yields (Scheme 1).

The coordination ability of Schiff-bases **7a,b** with Zn^{2+} ion was examined in an aqueous metanolic solution. The elemental analysis results (Experimental section) and the stoichiometry of the deep green complexes which was obtained by Job's method (Figs. S1 and S2, Supplementary Data) [23], proposed the [$Zn(L_2)_2$].N_2O_6 2(H_2O) formulae for the complexes (Scheme 3). Furthermore, molecular ion peak at m/z 954 ($[Zn(L1)_2]^{2+}$) and m/z 990 ($[Zn(L2)_2]^{2+}$) strongly support the structure of the new complexes.

Photophysical properties of the new ligands and complexes

Compounds **7a,b,** and Zinc complexes **8a,b** were spectrally characterized by UV-Vis and fluorescence spectroscopy in the wavelength range of 200–1000 nm.

The absorption and fluorescence emission spectra of the ligands **7a,b** and Zinc (II) complexes **8a,b** are shown in Figs. 1 and 2, respectively whereas numerical spectral data are presented in Table 1. Values of extinction coefficient (ε) were calculated as the slope of the plot of absorbance *vs* concentration. As depicted in Fig. 1, the spectra of complexes have an absorption maximum at 650 nm at which the ligand has no absorbance. An efficient charge transfer of an electron from p-orbital on the ligand to Zn (II) d-orbital can be considered as the main reason for the color of the complexes described as Ligand to-Metal Charge Transfer (LMCT) [24]. Also, Schiff-base ligands **7a,b,** and Zn complexes **8a,b** produced

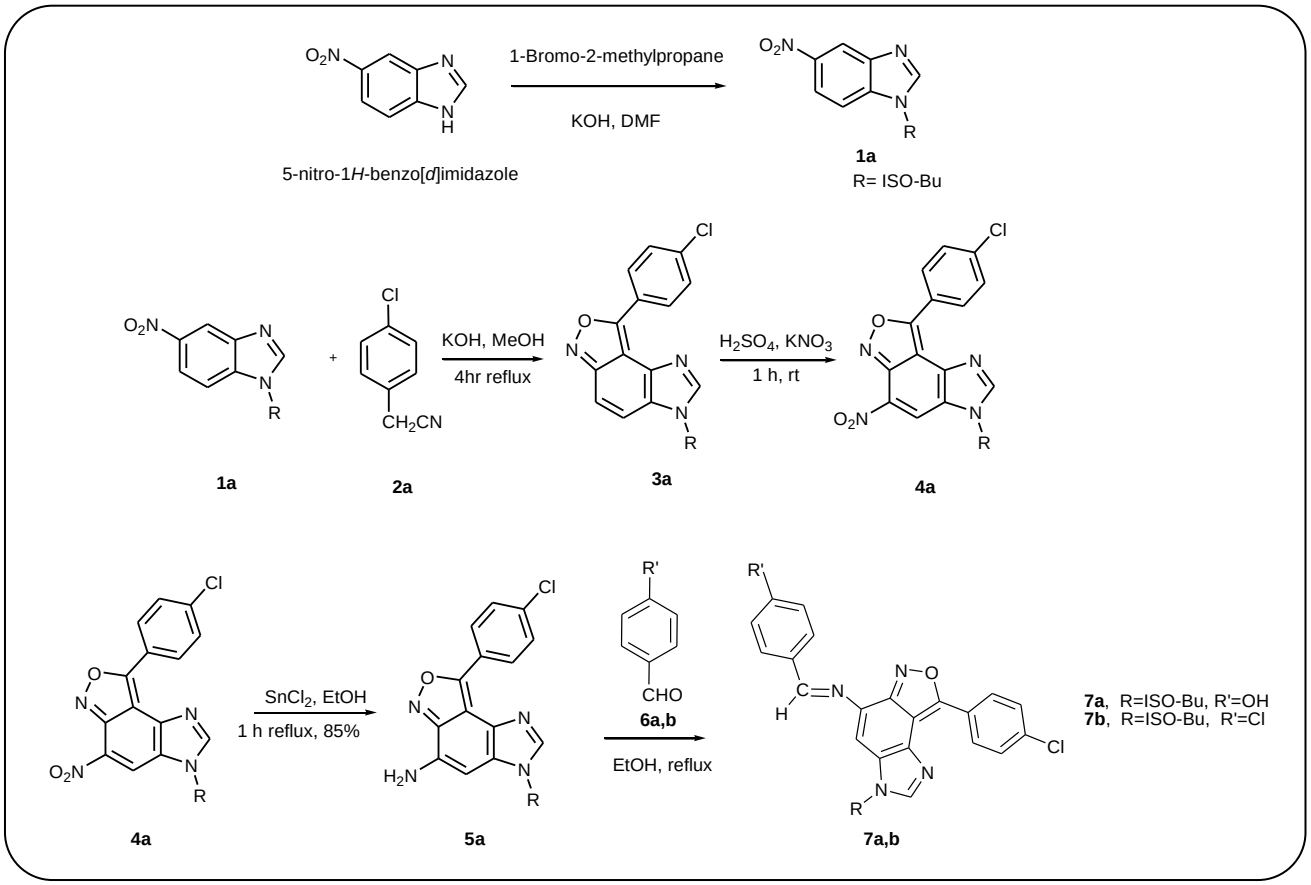

Scheme 1: Synthesis of the new ligands 7a,b.

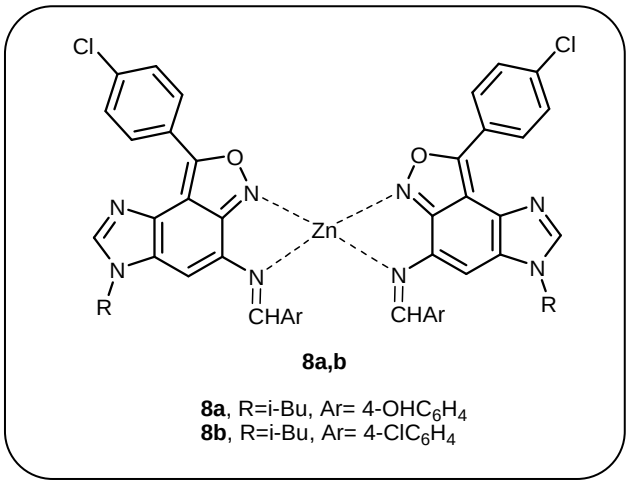

Scheme 2: The structure of the Zn(II) complexes 8a,b.

fluorescence at concentration 1×10^{-5} M in MeOH (Fig. 2). The fluorescence quantum yield of the compounds was determined *via* comparison methods, using fluorescein as a standard sample in 0.1 M NaOH and MeOH solution [25]. The used value of the fluorescein emission quantum yield is 0.79 and the obtained emission quantum yields of the new compounds are around 0.18 – 0.47. As can be seen from Table 1, extinction coefficient (ε) in Schiff-base **7b**, fluorescence intensity and the emission quantum yield in Schiff-base **7a** were the biggest values.

DFT calculation

According to reported literature [26] and our experimental results, an octahedral geometry was proposed for the Zinc complexes **8a,b**. To gain a deeper insight into the geometries and role of HOMO and LUMO frontier orbitals in the UV-visible absorption spectra of Schiff-bases **7a,b** and Zinc complexes **8a,b**, we performed DFT calculations at the B3LYP/6-311+G(d,p) level and obtained the optimized geometries and HOMO and LUMO frontier orbitals of fluorescent ligands **7a,b** and Zn(II) complex **8b**. The geometry of the complex **8b** was optimized in both of the gas phase and the PCM model, where the methanol was the used solvent. The optimized geometry of the ligands **7a,b** can be found in Fig. 3. The optimized geometry of the complex **8b** with labeling of its atoms is also depicted in Fig. 4 in two different views.

Table 1: Spectroscopic data for the new compounds 7a,b and 8a,b at 298 K.

Dye	7a	7b	8a	8b
λ_{abs} (nm)[a]	449	350	650	650
$\varepsilon \times 10^{-3}$ [(mol L^{-1})$^{-1}$$cm^{-1}$] [b]	5.00	5.20	3.70	2.90
λ_{flu} (nm)[c]	570	560	550	550
Φ_F[d]	0.39	0.47	0.18	0.23

a) Wavelengths of maximum absorbance (λ_{abs}); b) Extinction coefficient
c) Wavelengths of fluorescence emission (λ_{flu}) with excitation at 400 nm; d) Fluorescence quantum yield

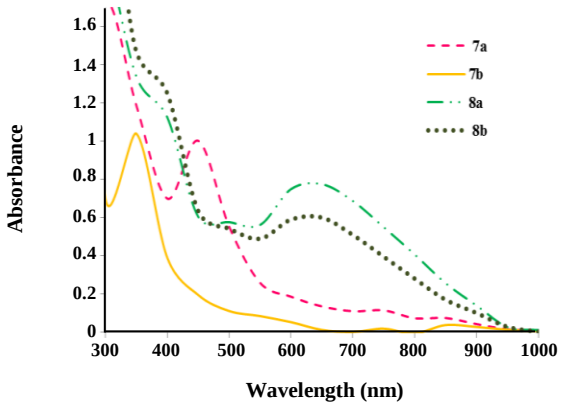

Fig. 1: The absorption spectra of the ligands 7a,b and Zn(II) complexes 8a,b in MeOH solution (2 × 10^{-4} M).

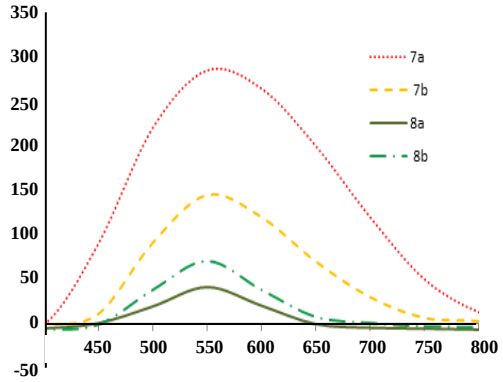

Fig. 2: The fluorescence emission spectra of the ligands 7a,b and Zn(II) complexes 8a,b in MeOH solution (1 × 10^{-5} M).

Some of the calculated structural parameters of the Zn(II) complex are collected in Table 2.

In the optimized geometry of the complex **8b**, the ligand **7b** acts as a bidentate ligand, coordinates to the Zn(II) *via* the nitrogen atom of the imine group (–N=CH) and nitrogen atom of the isoxazole ring.

Except for the Iso butyl group, the ligands **7b** are planar. The aromatic rings of the ligand are in the same plane. Also, both of the ligands are in the same plane forming a square plane of the tetrahedral complex. The Zn-O and Zn-N Lengths bonds are listed in Table 2.

The DFT computed ^{1}H NMR chemical shifts (δ) of Zn (II) complex **8b** are listed in Table 3 together with the experimental values for comparison. The atoms are numbered as in Fig. 4.

As seen in Table 3, the DFT-calculated NMR chemical shifts are in good agreement with the experimental values, confirming the suitability of the optimized geometries for Zn (II) complex **8b**.

Moreover, the vibrational modes of Zn complex **8b** were analyzed by comparing the experimental and DFT-computed IR spectra. The assignment of the selected-vibrational frequencies is gathered in Table 4. There is good agreement between the experimental and DFT-calculated frequencies of the high spin complex, confirming the validity of the optimized geometry as a proper structure for the complex **8b**.

The 3D-distribution map for the Highest-Occupied-Molecular Orbital (HOMO) and the Lowest-Unoccupied-Molecular Orbital (LUMO) of the ligands **7a,b** and the complex **8b** are shown in Fig. 5. As seen, the HOMO orbital of the ligands is localized on the benzimidazole and isoxazole rings. But the LUMO orbital is mainly localized on the benzene ring and its substitutions. Since, in the ligands **7a,b,** electron transition from the HOMO orbital to the LUMO orbital is $\pi \rightarrow \pi^*$ transition. On the other hand, the HOMO and LUMO frontier orbitals of the complex **8b** species are mainly localized on the isoxazole ring and Zn atom, respectively. It implies that the electron transition from the HOMO orbital to the LUMO orbital is Ligand to-Metal Charge Transfer (LMCT) [24].

The energy difference between the HOMO and LUMO frontier orbitals is one of the important characteristics of molecules, which has a determining role in such cases as electric properties, electronic spectra, and photochemical reactions. Energy separation between the HOMO and LUMO ($\Delta\varepsilon = \varepsilon_{LUMO} - \varepsilon_{HOMO}$) of **7a**, **7b**

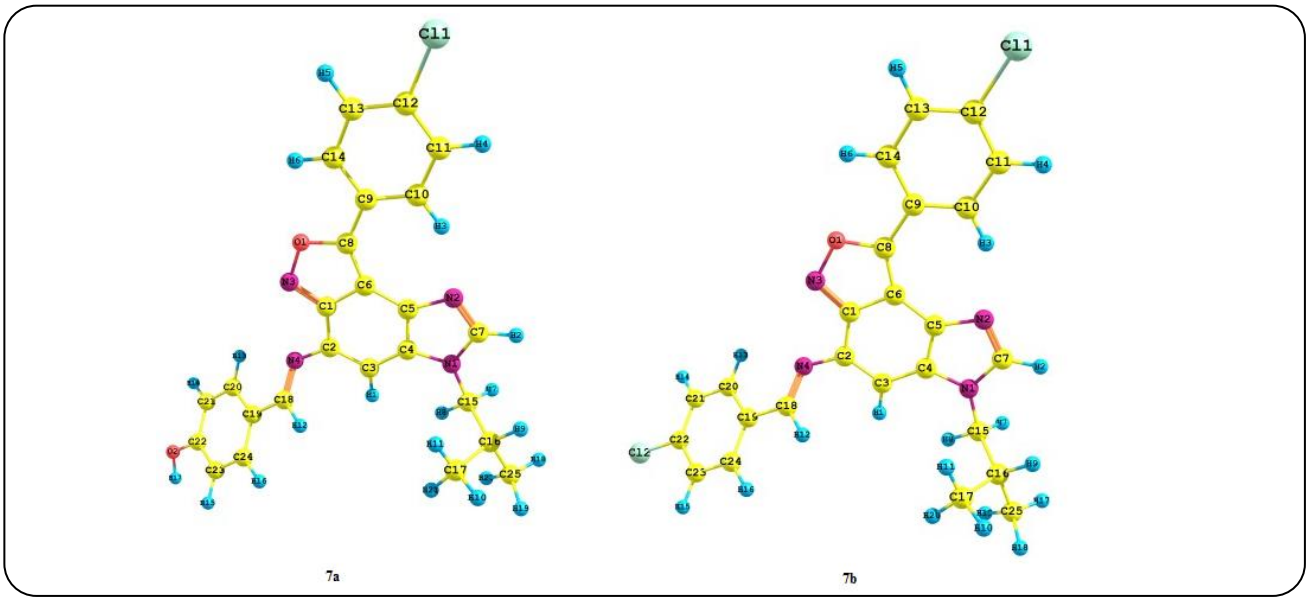

Fig. 3: The optimized geometry of the ligands 7a,b.

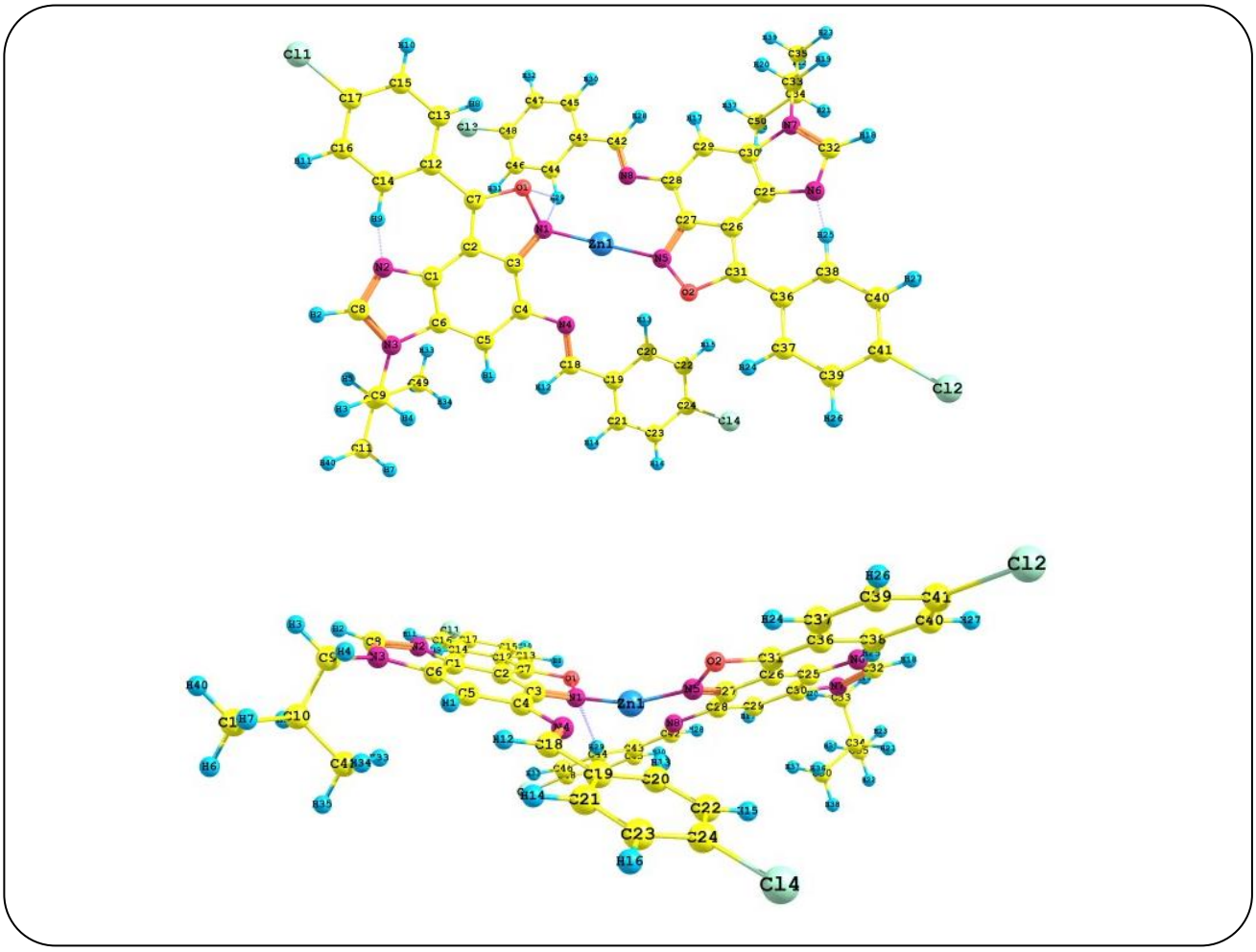

Fig. 4: The optimized geometry of the Zinc(II) complex 8b in two different views.

Table 2: Selected structural parameters of Zn (II) complex 8b.

Bond	Bond length (A^0)	Angle	(°)	Dihedral angle	(°)
Zn-N1	1.79	N1- Zn -N5	163.3	N1-N5-N4-N8	31.15
Zn -N4	2.74	N1- Zn -N4	80.3	N1-N5-N4-Zn	10.7
Zn -N5	1.89	N5- Zn -N8	88.4	O2-N5- Zn –N4	-40.1
Zn -N8	2.41	N1- Zn -N8	97.15	O2-N5- Zn –N1	55.5
N1 –O1	1.40	N4- Zn -N5	101.7	O2-N5- Zn -N8	165.5
C8-N2	1.32	N1- O1 –C7	102.3	C27-C28- N8-C42	178.3
N5-O2	1.40	N5- O2-C31	102.4	C27-N5- O2-C31	-11.14
O2-C31	1.44	N7- C32-N6	110.8	C27-C28-N8-C42	178.3
C31-C36	1.40	N7- C30-C29	131.3	C27-N5- Zn –N1	-101.0
C26-C27	1.35	C29-C28-N8	120.7	N8-C27-C27-N5	0.57
C27-C28	1.41	N8-C42-C43	120.4	O1-C7-C2-C3	-7.1
C28-C29	1.42	N8-C28-C27	121.2	O1-C7-C12-C13	0.19
C29-C30	1.40	C3-N1- Zn	116.0	C7-C2-C1-N2	-0.63
C30 –N7	1.44	Zn -N1-O1	126.8	C6-C1-N2-C8	0.17
N7-C32	1.34	C3-N1-O1	110.3	N2-C8- N3-C9	179.7
C32-N6	1.36	C4-N4-C18	119.4	C2-C7-C12-C13	-179.3
N6 -C25	1.35	N4-C18-C19	120.3	N6-C27-C28-C29	-179.3
N7-C33	1.46	C22.C24.Cl4	120.0	C1-C6-N3-C9	-179.6
N1-C3	1.34	C6-N3-C9	127.4	C3-C4-C5-C6	0.22
N8-C42	1.29	C1-N2-C8	107.5	N3-C9-C10-C11	179.8

Table 3: DFT calculated and experimental ^1H NMR chemical shifts of Zn (II) complex 8b in DMSO solution, δ [ppm].

Atomic number	Chemical shift		Atomic number	Chemical shift	
	Cal.	Exp.		Cal.	Exp.
H09	9.15	9.04	H02	7.67	7.58
H15	8.98	8.84	H19	4.11	4.27
H20	8.19	8.33	H25	1.68	1.62–1.64
H31	7.75	7.77	H27	1.35	1.19–1.21
H13	7.69	7.62	H34	0.92	0.85
H21	7.48	7.68			

Table 4: Selected experimental and calculated IR vibrational frequencies (cm^{-1}) of Zn(II) complex 8b.

Experimental frequency	Calculated frequency	Intensity (km/mol)	Vibrational assignment
525 (w)	536	65	υ_{sym}(Zn-N)
537 (w)	552	178	υ_{asym}(Zn-N)
834(s)	832	93	υ_{sym} (C-Cl) of the benzene rings involving the –Cl substituent
965(w)	906	154	$\delta_{wagging}$ of the $–CH_2$ moieties
	935	1131	Breathing of the aromatic rings
1025 (m)	962, 967	183, 224	υ(N1-O1, N5-O2)+ υ(C-C) aliphatic
	1012	105	υ(C31-N6, C8-N3)
1046 (s)	1043	938	υ(C32-N7, C31-N6)+ υ(C-Cl) + υ(C-O)
	1057, 1075	1081, 1279	υ(C-Cl) + υ_{asym}(C7-O1-N1, C30-O2-N5)
1078 (s)	1083	147	υ_{sym}(C-C) aliphatic
	1118	36	δ_{ip}(Aromatic hydrogens)
1176 (m, sh)	2008	435	υ(C4-N4, C27-N8, C7-O1, C30-O2)
	1119	667	υ(C2-C7, C30-C25)
1227 (m)	1216	218	υ(C7-O1, C30-O2)
1273(m)	1246	671	υ(C9-N3, C32-N7)
	1269	122	υ_{asym}(C1-N2-C8, C24-N6-C31)
1323 (m)	1315	2763	υ(C29-N7, C6-N3)
1361 (s)	1387	1527	υ(C=C, C=N) of the aromatic rings
1451 (vs)	1395	821	υ(C=C, C=N) of the aromatic rings
	1435	89	$\delta_{oscissoring}$ of the methyl groups
	1464	183	$\delta_{oscissoring}$ of the $–CH_2$ moieties
1484 (vs, sh)	1486	85	υ_{asym}(C-C) of the benzene rings involving the –Cl substituent
	1483	78	
1577(vs)	1537	1985	υ(C=C, C=N) of the aromatic rings
	1558	3993	
	1566	1084	
1646(m)	1636	61	υ_{asym} (C=N) of the imine
2881 (w)	2885, 2968	58,16	υ_{sym}(C-H) of the $–CH_2$ moieties
2911(m)	2874	63	υ_{sym}(C-H) of the methyl groups
2906(m)	2883-2947	8-42	υ_{asym}(C-H) of the $–CH_2$ moieties
2971 (w)	2949 -2989	13-46	υ(C-H) aromatic
	3046	89	υ(C8-H2, C31-H15)

Abbreviation: op, out-of-plane; ip, in-plane; w, weak; m, medium; s, strong; vs, very strong; br, broad; sh, shoulder.

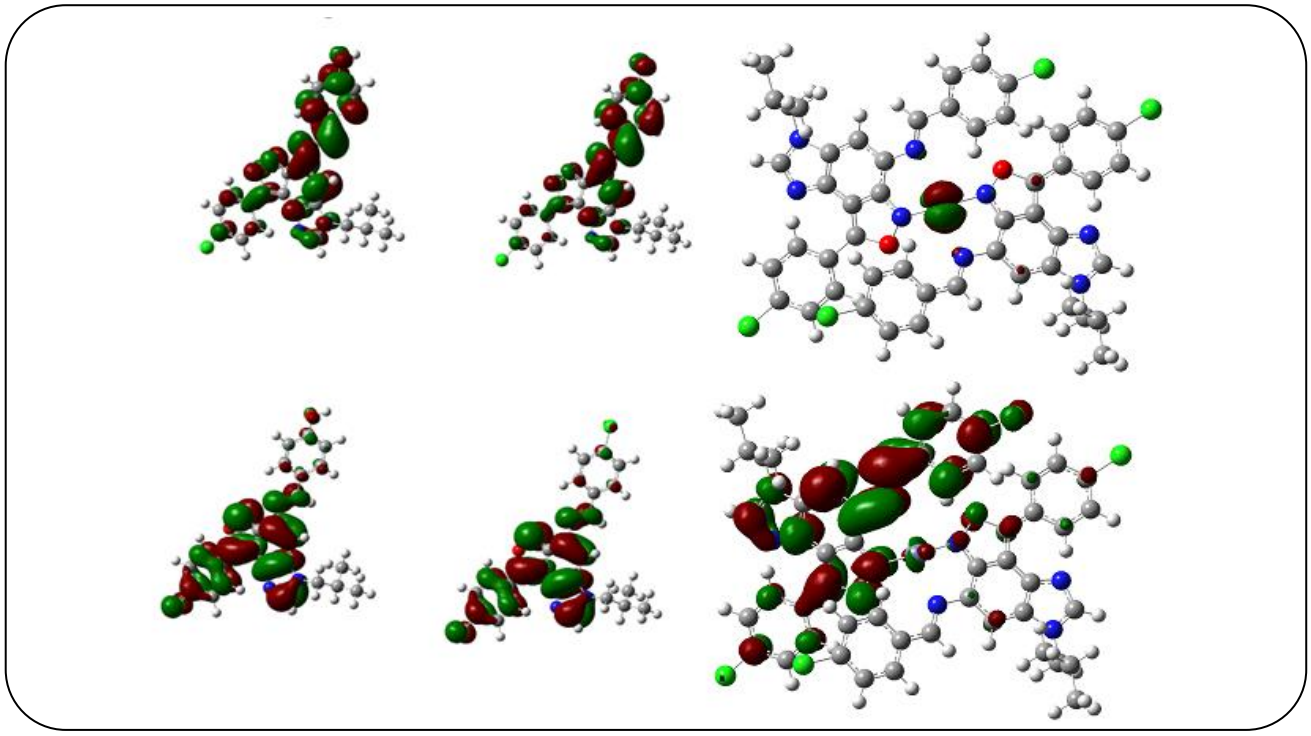

Fig. 5: The HOMO (down) and LUMO (up) frontier orbitals of the ligands 7a,b, and complex 8b.

and **8b** is 3.16 eV (420 nm), 3.23 eV (327 nm) and 2.70 eV (610 nm), compared with the experimental values of 449, 350 and 650 nm respectively.

Antibacterial studies

The antibacterial activity of the ligands **7a,b,** and complexes **8a,b** was tested against a panel of strains of Gram negative bacterial (*Pseudomonas aeruginosa* (ATCC 27853) and *Escherichia coli*, (ATCC 25922)) and Gram positive (*Staphylococcuse aureus methicillin resistant S. aureus* (MRSA) clinical isolated and *Bacillus subtilis* (ATCC 6633)) species (Table 5) using broth microdilution method as previously described [27]. A comparison with Ampicillin as a standard was done. The lowest concentration of the antibacterial agent that prevents the growth of the test organism, as detected by a lack of visual turbidity (matching the negative growth control), is designated the minimum inhibitory concentration (MIC). Experimental details of the tests can be found in our earlier study [28].

As seen in Table 5, compounds **7a,b** inhibit the metabolic growth of the tested Gram positive and negative bacteria to the same extent, but the inhibitions percent are less than those of Ampicillin. Coordination of ligands **7a,b** to Zn(II) leads to an improvement in the antibacterial agent. This can be explained by Tweed's chelation theory [29, 30], which explicated that the lipophilicity of the uncoordinated ligand could be changed by reducing the polarizability of the M^{n+} ion *via* the L→M donation, and the possible electron delocalization over the metal complexes. Also, the results revealed that the complex **8a** with R= Iso bu and Ar= 4-OHC_6H_4 groups, displayed greater antibacterial activity against Gram-negative bacteria than did the well known antibacterial agent Ampicillin (Table 5).

CONCLUSIONS

In summary, we have synthesized two new fluorescent heterocyclic Schiff base ligands from the reaction of 8-(4-chlorophenyl)-3-iso-butyl-3*H*-imidazo[4',5':3,4]benzo [1,2-*c*]isoxazol-5-amine with *p*-hydroxybenzaldehyde and *p*-chlorobenzaldehyde. Coordination of the ligands with Zn(II) cation led to the formation of deep green complexes in high yields. The structures of the complexes have been confirmed by spectral, analytical data and Job's method. Schiff-base ligands and Zinc complexes were spectrally characterized by UV-Vis and fluorescence spectroscopy. In addition, the DFT methods were employed to achieve deeper insight into geometry and spectral properties of the synthesized compounds. The DFT-calculated spectral properties are in good agreement with the experimental

Table 5: Antibacterial activity (MIC, μg mL^{-1}) of reference and compounds 7a, b and 8a,b.

Compds.	S.a. (MRSA)	B.s. (ATCC 6633)	P.a. (ATCC 27853)	E.c. (ATCC 25922)
7a	80	80	80	85
7b	100	100	95	95
8a	30	25	20	5
8b	45	35	25	10
Ampicillin	62	0.50	125	8

values, confirming the suitability of the optimized geometries for Zn(II) complexes. Moreover, results from the antimicrobial screening tests show that new compounds are effective against standard strains of Gram-negative growth inhibitors. An improvement in the antibacterial agent is observed upon the coordination of the Zn(II) ion.

Acknowledgment

We would like to express our sincere gratitude to the Research Office, Mashhad Branch, Islamic Azad University, Mashhad-Iran, for financial support of this work. We must also acknowledge Dr. Mehdi Pordel for his valuable guidance (Department of Chemistry, Mashhad Branch, Islamic Azad University, Mashhad, Iran).

Received : Feb. 14, 2018 ; Accepted :Jun. 18, 2018

REFERENCES

[1] Ashraf M.A., Maah M.J., Yusuf I., Synthesis, Characterization and Biological Studies of 2-(4-Nitrophenylaminocarbonyl) Benzoic Acid and Its Complexes with Cr (III), Co (II), Ni (II), Cu (II) and Zn (II), *Iran. J. Chem. Chem. Eng. (IJCCE)*, **31**(1): 9-14 (2012).

[2] Parekh H., Patel M., Preparation of Schiff's Base Complexes of Mn (II), Co (II), Ni (II), Cu (II), Zn (II), and Cd (II) and Their Spectroscopic, Magnetic, Thermal, and Antifungal Studies, *Russ. J. Coord. Chem.*, **32**(6): 431-436 (2006).

[3] Neelakantan M., Rusalraj F., Dharmaraja J., Johnsonraja S., Jeyakumar T., Pillai M.S., Spectral Characterization, Cyclic Voltammetry, Morphology, Biological Activities and DNA Cleaving Studies of Amino Acid Schiff Base Metal (II) Complexes, *Spectrochim. Acta A Mol. Biomol. Spectrosc.*, **71**(4): 1599-1609 (2008).

[4] Kovala-Demertzi D., Yadav P.N., Wiecek J., Skoulika S., Varadinova T., Demertzis M.A., Zinc (II) Complexes Derived from Pyridine-2-Carbaldehyde Thiosemicarbazone and (1E)-1-pyridin-2-ylethan -1-one Thiosemicarbazone. Synthesis, Crystal Structures and Antiproliferative Activity of Zinc (II) Complexes, *J. Inorg. Biochem.*, **100**(9): 1558-1567 (2006).

[5] Payehghadr M., Taghdiri M., Zamani A., Hesaraki N., Conductometric Studies of the Thermodynamics of Complexation of Zn^{2+}, Ni^{2+}, Co^{2+}, Pb^{2+}, Mn^{2+}, Cu^{2+} Ions with 1, 13-Bis (8-Quinolyl)-1, 4, 7, 10, 13-Pentaoxatridecane in Binary Solvent Mixtures, *Iran. J. Chem. Chem. Eng.*, **31**(3): 1-7 (2012).

[6] Yue S.-M., Xu H.-B., Ma J.-F., Su Z.-M., Kan Y.-H., Zhang H.-J., Design and Syntheses of Blue Luminescent Zinc(II) and Cadmium(II) Complexes with Bidentate or Tridentate Pyridyl-imidazole Ligands, *Polyhedron*, **25**(3): 635-644 (2006).

[7] Hoogenraad T., Koevoet R., de Ruyter Korver E., Oral Zinc Sulphate as Long-Term Treatment in Wilson's Disease (Hepatolenticular Degeneration), *Eur. Neurol.*, **18**(3): 205-211 (1979).

[8] Pinilla-Tenas J.J., Sparkman B.K., Shawki A., Illing A.C., Mitchell C.J., Zhao N., Liuzzi J.P., Cousins R.J., Knutson M.D., Mackenzie B., Zip14 is a Complex Broad-Scope Metal-Ion Transporter Whose Functional Properties Support Roles in the Cellular Uptake of Zinc and Nontransferrin-Bound Iron, *Am. J. Physiol., Cell Physiol.*, **301**(4): C862-C871 (2011).

[9] Szarfman A., Tonning J.M., Levine J.G., Doraiswamy P.M., Atypical Antipsychotics and Pituitary Tumors: A Pharmacovigilance Study, *Pharmacotherapy*, **26**(6): 748-758 (2006).

[10] Deng B.-L., Zhao Y., Hartman T.L., Watson K., Buckheit R.W., Pannecouque C., De Clercq E., Cushman M., Synthesis of Alkenyldiarylmethanes (ADAMs) Containing Benzo [d] Isoxazole and Oxazolidin-2-one Rings, A New Series of Potent Non-Nucleoside HIV-1 Reverse Transcriptase Inhibitors, *Eur. J. Med. Chem.*, **44**(3): 1210-1214 (2009).

[11] Loudon J., Tennant G., Substituent Interactions in Ortho-Substituted Nitrobenzenes, *Chem. Soc. Rev.*, **18**(4): 389-413 (1964).

[12] Munsey M.S., Natale N.R., The Coordination Chemistry of Isoxazoles, *Coord. Chem. Rev.*, **109**(2): 251-281 (1991).

[13] Güngör Ö., Gürkan P., Synthesis and Characterization of Higher Amino Acid Schiff Bases, as Monosodium Salts and Neutral Forms. Investigation of the Intramolecular Hydrogen Bonding in All Schiff Bases, Antibacterial and Antifungal Activities of Neutral Forms, *J. Mol. Struct.*, **1074** (Supplement C): 62-70 (2014).

[14] Joux F., Lebaron P., Use of Fluorescent Probes to Assess Physiological Functions of Bacteriaat Single-Cell Level, *Microbes Infect.*, **2**(12): 1523-1535 (2000).

[15] Preston P.N., "The Chemistry of Heterocyclic Compounds, Benzimdazoles and Cogeneric Tricyclic Compounds", John Wiley & Sons, Inc., Vol. 40 (2009).

[16] Rahimizadeh M., Pordel M., Bakavoli M., Bakhtiarpoor Z., Orafaie A., Synthesis of Imidazo[4,5-a]acridones and Imidazo[4,5-a]acridines as Potential Antibacterial Agents, *Monatsh. Chem.*, **140**(6): 633- (2009).

[17] Ramezani S., Pordel M., Beyramabadi S., Synthesis, Spectroscopic Characterization and DFT/TD-DFT Calculations of New Fluorescent Derivatives of Imidazo[4′,5′:3,4]Benzo[c]Isoxazole, *J. Fluoresc.*, **26**(2): 513-519 (2016).

[18] Agheli Z., Pordel M., Beyramabadi S.A., New Fe(III) Complex with 8-(4-chlorophenyl)-3-butyl-3H-imidazo[4′,5′:3,4]benzo[1,2-c]isoxazol -5-amine (5-AIBI) Ligand: Synthesis, Spectroscopic Characterization and DFT Calculations, *J. Mol. Struct.*, **1130**(Supplement C): 55-61 (2017).

[19] Lee C., Yang W., Parr R.G., Development of the Colle-Salvetti Correlation-Energy Formula into a Functional of the Electron Density, *Phys. Rev. B*, **37**(2): 785- 789 (1988).

[20] Frisch M., Trucks G., Schlegel H., Scuseria G., Robb M., Cheeseman J., Montgomery Jr J., Vreven T., Kudin K., Burant J., Gaussian 03, Revision B. 03, Gaussian, Inc., Wallingford, CT, 2004. Gaussian 03, Revision B. 05, MJ Frisch, et al. Gaussian, Inc., Pittsburgh, *PA*: (2003).

[21] Cammi R., Tomasi J., Remarks on the Use of the Apparent Surface Charges (ASC) Methods in Solvation Problems: Iterative Versus Matrix-Inversion Procedures and the Renormalization of the Apparent Charges, *J. Comput. Chem.*, **16**(12): 1449-1458 (1995).

[22] Rezazadeh M., Pordel M., Davoodnia A., Saberi S., New Fluorescent 3H-imidazo [4, 5-e][2, 1] Benzoxazoles: Synthesis, Spectroscopic Characterization, and Antibacterial Activity, *Chem. Heterocycl. Compd.*, **51**(10): 918-922 (2015).

[23] Vosburgh W.C., Cooper G.R., Complex ions. I. The Identification of Complex Ions in Solution by Spectrophotometric Measurements, *J. Am. Chem. Soc.*, **63**(2): 437-442 (1941).

[24] Saureu S., de Graaf C., TD-DFT Study of the Light-Induced Spin Crossover of Fe(iii) Complexes, *Phys. Chem. Chem. Phys.* , **18**(2): 1233-1244 (2016).

[25] Umberger J.Q., LaMer V.K., The Kinetics of Diffusion Controlled Molecular and Ionic Reactions in Solution as Determined by Measurements of the Quenching of Fluorescence1,2, *J. Am. Chem. Soc.*, **67**(7): 1099-1109 (1945).

[26] Preti C., Tosi G., Massacesi M., Ponticelli G., Chromium (III) Halide Complexes with Isoxazole and Substituted Isoxazoles as Ligands, *Spectrochim. Acta A Mol. Biomol. Spectrosc.*, **32**(12): 1779-1784 (1976).

[27] Tezer N., Karakus N., Theoretical Study on the Ground State Intramolecular Proton Transfer (IPT) and Solvation Effect in Two Schiff Bases Formed by 2-aminopyridine with 2-hydroxy-1- naphthaldehyde and 2-hydroxy Salicylaldehyde, *J. Mol. Model.* , **15**(3): 223-232 (2009).

[28] Pordel M., Abdollahi A., Razavi B., Synthesis and Biological Evaluation of Novel Isoxazolo[4,3-e]indoles as Antibacterial Agents, *Russ. J. Bioorg. Chem.*, **39**(2): 211-214 (2013).

[29] Tweedy B., Plant Extracts with Metal Ions as Potential Antimicrobial Agents, *Phytopathology*, **55**: 910-914 (1964).

[30] Nakhaei A., Davoodnia A., Yadegarian S., Application of ZrO_2–SO_3H as Highly Efficient Recyclable Nano-Catalyst for the Green Synthesis of Fluoroquinolones as Potential Antibacterial, *Iran. Chem. Commun.*, **6**(4): 6-15 (2018).